

# Constraining wrong-sign $hbb$ couplings with $h \rightarrow \Upsilon\gamma$

Tanmoy Modak,<sup>1,\*</sup> Jorge C. Romão,<sup>2,†</sup> Soumya Sadhukhan,<sup>1,‡</sup> João P. Silva,<sup>2,§</sup> and Rahul Srivastava<sup>1,3,¶</sup>

<sup>1</sup>*The Institute of Mathematical Sciences, Chennai, India*

<sup>2</sup>*CFTP, Departamento de Física, Instituto Superior Técnico,  
Universidade de Lisboa, Avenida Rovisco Pais 1, 1049 Lisboa, Portugal*

<sup>3</sup>*Physical Research Laboratory, Ahmedabad, India*

(Dated: August 13, 2018)

The rare decay  $h \rightarrow \Upsilon\gamma$  has a very small rate in the Standard Model, due to a strong cancellation between the direct and indirect diagrams. Models with a changed  $hbb$  coupling can thus lead to a great increase in this decay. Current limits on two Higgs doublet models still allow for the possibility that the  $hbb$  coupling might have a sign opposite to the Standard Model; the so-called “wrong-sign”. We show how  $h \rightarrow \Upsilon\gamma$  can be used to put limits on the wrong-sign solutions.

PACS numbers: 12.60.Fr, 14.80.Ec, 14.80.-j

## I. INTRODUCTION

With the discovery at LHC of the first spin 0 particle [1, 2], one must now probe its couplings in detail, searching for discrepancies with the Standard Model (SM) Higgs. Of particular interest is the possibility that the  $hbb$  coupling could have a magnitude close to the SM value, but opposite sign; the “wrong-sign” solution. Current data is consistent with this possibility [3–5].

There is great interest in the two Higgs doublet model (2HDM) [6, 7]. Most attention is devoted to models with a discrete  $Z_2$  symmetry, softly broken by a term with a real coefficient. These models have two charged scalars  $H^\pm$ , one pseudoscalar  $A$ , a heavy scalar  $H$ , and a light scalar  $h$ , which we identify as the 125 GeV scalar from LHC. There are four types of such models. Of these, only Type II and Flipped are consistent with wrong-sign solutions [8–10].

Naturally, a sign change does not affect the  $h \rightarrow b\bar{b}$  rate, which, in most models of the 125 GeV scalar, is very close to its total width. Thus, the effect of the wrong-sign must be sought indirectly, for example through its one-loop contribution to the glue-gluon production  $gg \rightarrow h$  and di-photon decay  $h \rightarrow \gamma\gamma$ . However, there, loops with intermediate bottom quarks compete with much larger contributions from loops with top quarks ( $gg \rightarrow h$ ) or with top quarks and with gauge bosons ( $h \rightarrow \gamma\gamma$ ). As a result, these processes will have values close to the SM, and only a very precise measurement of order 5% in  $pp \rightarrow h \rightarrow \gamma\gamma$  will enable experiments to disentangle the normal sign from the wrong-sign solutions [9, 11].

In contrast, the rare decay  $h \rightarrow \Upsilon\gamma$  involves two diagrams which have almost the same magnitude in the SM. The decay is very suppressed in the SM (compared, for example, with  $h \rightarrow J/\psi\gamma$ ) due to an accidental cancellation between the two diagrams [12, 13]. A change in the  $hbb$  sign will destroy the precise cancellation and will have a dramatic effect in this decay, making  $h \rightarrow \Upsilon\gamma$  the prime candidate to probe the wrong-sign solutions. The importance of such a measurement on the wrong-sign solutions of the 2HDM is the subject of this article.

In Section II we introduce our notation, and in Section III we present the details of the  $h \rightarrow \Upsilon\gamma$  decay and perform a full simulation within the real 2HDM. In Section IV we draw our conclusions.

---

\*E-mail: tanmoy@imsc.res.in

†E-mail: jorge.romao@tecnico.ulisboa.pt

‡E-mail: soumyasad@imsc.res.in

§E-mail: jpsilva@cftp.ist.utl.pt

¶Email: rahuls@prl.res.in

## II. WRONG-SIGN SOLUTION IN THE 2HDM

### A. Notation

In this article we consider a CP-conserving 2HDM with a discrete  $Z_2$  symmetry, broken softly by a real term, reviewed extensively for example in [6, 7]. The scalar potential may be written as

$$\begin{aligned}
V_H = & m_{11}^2 |\Phi_1|^2 + m_{22}^2 |\Phi_2|^2 - m_{12}^2 \left[ \Phi_1^\dagger \Phi_2 + \Phi_2^\dagger \Phi_1 \right] \\
& + \frac{\lambda_1}{2} |\Phi_1|^4 + \frac{\lambda_2}{2} |\Phi_2|^4 + \lambda_3 |\Phi_1|^2 |\Phi_2|^2 + \lambda_4 (\Phi_1^\dagger \Phi_2) (\Phi_2^\dagger \Phi_1) \\
& + \frac{\lambda_5}{2} \left[ (\Phi_1^\dagger \Phi_2)^2 + (\Phi_2^\dagger \Phi_1)^2 \right], \tag{1}
\end{aligned}$$

with all coefficients real. The vacuum expectation values (vevs) are also real and written as  $v_1/\sqrt{2}$  and  $v_2/\sqrt{2}$ . The fields may be parametrized in terms of the mass eigenstates as

$$\begin{aligned}
\Phi_1 = & \left( \begin{array}{c} c_\beta G^+ - s_\beta H^+ \\ \frac{1}{\sqrt{2}} [vc_\beta + (-s_\alpha h + c_\alpha H) + i(c_\beta G^0 - s_\beta A)] \end{array} \right), \\
\Phi_2 = & \left( \begin{array}{c} s_\beta G^+ + c_\beta H^+ \\ \frac{1}{\sqrt{2}} [vs_\beta + (c_\alpha h + s_\alpha H) + i(s_\beta G^0 + c_\beta A)] \end{array} \right), \tag{2}
\end{aligned}$$

where  $c_\theta$  ( $s_\theta$ ) is the cosine (sine) of any angle  $\theta$  in subscript,  $\tan \beta = v_2/v_1$ , and  $v = \sqrt{v_1^2 + v_2^2} = (\sqrt{2}G_F)^{-1/2}$ . The fields  $G^\pm$  and  $G^0$  are the would-be Goldstone bosons.

We assume that the lightest scalar ( $h$ ) is the 125 GeV resonance found at LHC. Its couplings with the gauge bosons are

$$\mathcal{L}_{hVV} = \sin(\beta - \alpha)h \left[ \frac{m_Z^2}{v} Z^\mu Z_\mu + 2 \frac{m_W^2}{v} W^{+\mu} W_\mu^- \right]. \tag{3}$$

The SM limit corresponds to  $\sin(\beta - \alpha) = 1$ . We are interested in models with wrong-sign solutions for the fermion couplings. Given current experiments, only Type II and Flipped are consistent with this possibility [8–10]. In these models, the couplings of  $h$  with the fermions from the third family are

$$-\mathcal{L}_{\text{Yuk}} = \frac{m_t}{v} k_U h \bar{t}t + \frac{m_b}{v} k_D h \bar{b}b + \frac{m_\tau}{v} k_\tau h \tau^+ \tau^-, \tag{4}$$

where

$$k_U = \frac{\cos \alpha}{\sin \beta}, \quad k_D = -\frac{\sin \alpha}{\cos \beta}. \tag{5}$$

The only difference between the Type II and Flipped models lies in the coupling of the charged fermions, given, respectively, by

$$k_\tau = k_D \text{ (Type II)}, \quad k_\tau = k_U \text{ (Flipped)}. \tag{6}$$

The SM limit is  $k_U = k_D = k_\tau = 1$ .

We will denote the ratios between the 2HDM and SM rates by

$$\mu_f = \frac{\sigma^{2\text{HDM}}(pp \rightarrow h) \Gamma^{2\text{HDM}}[h \rightarrow f] \Gamma^{\text{SM}}[h \rightarrow \text{all}]}{\sigma^{\text{SM}}(pp \rightarrow h) \Gamma^{\text{SM}}[h \rightarrow f] \Gamma^{2\text{HDM}}[h \rightarrow \text{all}]}, \tag{7}$$

where  $\sigma$  is the cross section for Higgs production,  $\Gamma[h \rightarrow f]$  the decay width into the final state  $f$ , and  $\Gamma[h \rightarrow \text{all}]$  is the total Higgs decay width.

### B. A naive explanation for the wrong-sign

For simplicity, let us assume that the production of  $h$  is due exclusively to the gluon fusion process with intermediate top quark, and that its width is due exclusively to the decay  $h \rightarrow b\bar{b}$ . Within these assumptions

$$\sqrt{\mu_{VV}} = \pm \frac{k_U}{k_D} \sin(\beta - \alpha), \quad (8)$$

where the sign (which will be ignored henceforth) is chosen to make the square root positive. Imagine that  $\mu_{VV} \sim 1$  because both factors are close to unity. We start by noting that

$$-\frac{k_U}{k_D} = \frac{1}{t_\alpha t_\beta} = \frac{\cos(\beta - \alpha) + \cos(\beta + \alpha)}{\cos(\beta - \alpha) - \cos(\beta + \alpha)}, \quad (9)$$

where  $t_\theta$  is the tangent of the angle  $\theta$ . We find that  $|k_U/k_D| \sim 1$  if  $\beta - \alpha = \pi/2$ , in which case  $k_D = +1$  (the right-sign solution), or else if  $\beta + \alpha = \pi/2$ , in which case  $k_D = -1$  (the wrong-sign solution).

Now, we look at the second factor in Eq. (8). We find

$$\frac{\sin(\beta - \alpha)}{\sin(\beta + \alpha)} = \frac{1 - \frac{t_\alpha}{t_\beta}}{1 + \frac{t_\alpha}{t_\beta}} = \frac{1 + \frac{1}{t_\beta^2} \frac{k_D}{k_U}}{1 - \frac{1}{t_\beta^2} \frac{k_D}{k_U}}. \quad (10)$$

For  $|k_U/k_D| \sim 1$ , if  $t_\beta$  is larger than about 3 (say), then

$$\sin(\beta - \alpha) \sim \sin(\beta + \alpha) \left[ 1 + \frac{2}{t_\beta^2} \frac{k_D}{k_U} \right]. \quad (11)$$

Thus, the second factor in Eq. (8) is very closely given by  $\sin(\beta + \alpha)$  already for moderate values of  $t_\beta$ . In conclusion, an experimental constraint of  $\mu_{VV} \sim 1$  has a solution  $\sin(\beta - \alpha) \sim 1$  for all values of  $t_\beta$ , and it also has a solution  $\sin(\beta + \alpha) \sim 1$  for values of  $t_\beta \gtrsim 3$ . As an illustration, we show in Fig. 1 the constraints on the  $\sin \alpha$ - $\tan \beta$  plane of a 20% precision measurement of  $\mu_{VV}$  around the SM value 1. The left branch corresponds to the right-sign and lies

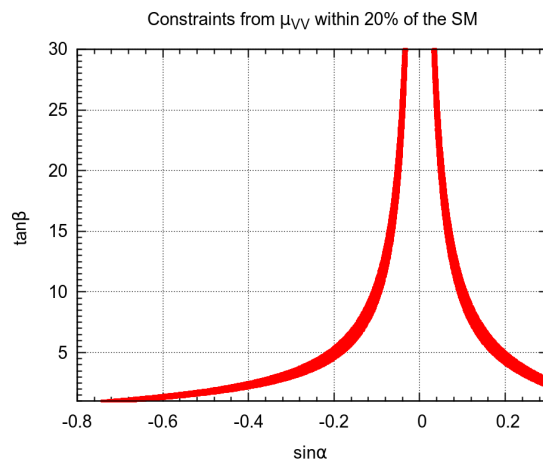


FIG. 1: Constraints from  $0.8 \leq \mu_{VV} \leq 1.2$  on the  $\sin \alpha$ - $\tan \beta$  plane.

very close to the line  $\sin(\beta - \alpha) = 1$  ( $k_D = 1$ ), while the right branch corresponds to the wrong-sign and lies very close to the line  $\sin(\beta + \alpha) = 1$  ( $k_D = -1$ ).

We note that, because both factors in Eq. (8) get closer to one in the right-sign and wrong-sign limits, a moderate precision in  $\mu_{VV}$  implies a very precise line in the  $\sin \alpha$ - $\tan \beta$  plane [11]. As shown in detail in section IIB of [11], for  $\tan \beta = 10$  and a precision of 20% in  $\mu_{VV}$ ,  $\sin^2(\beta - \alpha)$  is determined to better than 0.5% in the wrong-sign branch.

### III. THE $h \rightarrow \Upsilon\gamma$ DECAY IN 2HDM

#### A. Decay rate

The  $h \rightarrow \Upsilon\gamma$  decay rate may be written as

$$\Gamma[h \rightarrow \Upsilon\gamma] = \frac{1}{8\pi} \frac{m_h^2 - m_\Upsilon^2}{m_h^2} |\mathcal{A}_{\text{direct}} + \mathcal{A}_{\text{indirect}}|^2. \quad (12)$$

The direct diagram is shown in Fig. 2(b) and arises from the direct  $hb\bar{b}$  coupling ( $k_D$ ). The indirect diagram is shown in Fig. 2(a) and arises from the effective  $h\gamma\gamma$  with a virtual photon morphing into an  $\Upsilon$ .

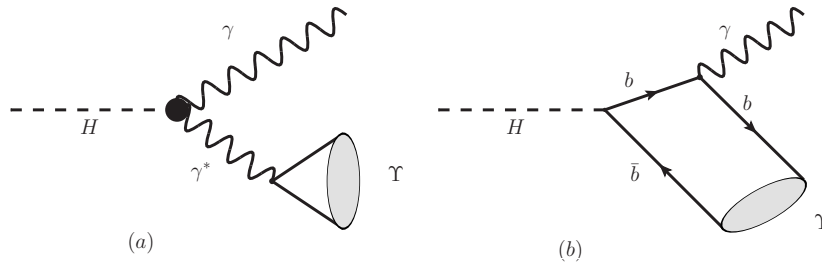


FIG. 2: Feynman diagrams contributing to the  $h \rightarrow \Upsilon\gamma$  process. The diagrams originate from two different couplings: (a) loop induced  $h\gamma\gamma$  (indirect) coupling; (b)  $hb\bar{b}$  Yukawa (direct) coupling.

We adapt the calculations of Ref. [12] to the 2HDM, and write

$$\begin{aligned} \mathcal{A}_{\text{direct}} &= -\eta \frac{2}{\sqrt{3}} e k_D \left( \sqrt{2} G_F \frac{m_\Upsilon}{m_h} \right)^{1/2} \frac{m_h^2 - m_\Upsilon^2}{m_h^2 - m_\Upsilon^2/2 - 2m_b^2} \phi_0(\Upsilon), \\ \mathcal{A}_{\text{indirect}} &= \frac{e g_{\Upsilon\gamma}}{m_\Upsilon^2} \left( \sqrt{2} G_F \right)^{1/2} \frac{\alpha}{\pi} \frac{m_h^2 - m_\Upsilon^2}{\sqrt{m_h}} \frac{X}{4}, \end{aligned} \quad (13)$$

where  $G_F$  is Fermi's constant,  $e$  is the positron charge,  $k_D$  is given in Eq. (5),  $m_\Upsilon$  and  $m_b$  are the  $\Upsilon$  and b-quark masses,  $\alpha$  is the fine-structure constant,  $\phi_0^2(\Upsilon) \sim 0.512 \text{ GeV}^3$  is the wave function of  $\Upsilon$  at the origin, and

$$g_{\Upsilon\gamma} = \frac{2}{\sqrt{3}} \sqrt{m_\Upsilon} \phi_0(\Upsilon), \quad (14)$$

whose magnitude can be determined from

$$\Gamma[\Upsilon \rightarrow \ell^+ \ell^-] = \frac{4\pi\alpha^2(m_\Upsilon)}{3m_\Upsilon^3} g_{\Upsilon\gamma}^2. \quad (15)$$

Our expressions in Eqs. (13) bear three differences with respect to Eqs. (14a)-(14b) of Ref. [12]. First, we have included explicitly in  $\mathcal{A}_{\text{direct}}$  the factor  $\eta = 0.689$  mentioned at the end of section IIA of [12], due to the full NLO corrections [12, 13]. Second, we have corrected in  $\mathcal{A}_{\text{indirect}}$  a  $\sqrt{2}$  misprint<sup>1</sup>. Finally, we have defined  $\mathcal{I} = -X/4$ , where  $X$  is the function arising from the calculation of the effective  $h\gamma\gamma$  coupling at one-loop in the 2HDM, which can be found in appendix B of Ref. [14].

As shown in [12], the direct and indirect contributions interfere destructively in an almost complete manner in the SM, and  $h \rightarrow \Upsilon\gamma$  cannot be detected. This is also the case in the right-sign solution of the 2HDM. In contrast, the wrong-sign solution has a constructive interference, raising the prospects for detection. This is what we turn to next.

<sup>1</sup> We are grateful to G. Bodwin for clarifications on this point. We agree with their Eq. (12), but have a  $\sqrt{2}$  difference with respect to their Eq. (14b).

## B. The importance of $h \rightarrow \Upsilon\gamma$ for the wrong-sign scenario

As mentioned, the experimental measurement of  $\mu_{VV}$  means that the  $hVV$  and  $ht\bar{t}$  couplings lie close to their SM values. As a result,  $h \rightarrow \gamma\gamma$  in the 2HDM is still dominated by the  $W$  loop, with a small destructive interference correction from the top loop. There are two novelties in the 2HDM. First, the alteration of  $k_D$ . The bottom loop contribution is negligible in the SM. It can indeed change sign in the 2HDM, but, since  $\mu_{VV}$  places  $|k_D| \sim 1$ , it cannot have a strong impact. Second, there is a charged Higgs loop. This decouples with the mass of the charged Higgs, but it can still give a contribution of up to ten percent for values of the charged Higgs mass around 600 GeV. Such effects are inevitable in the wrong-sign scenario [9]. One concludes that only precise measurements of the  $h \rightarrow \gamma\gamma$  decays can yield a signal for the wrong-sign solution of the 2HDM [9, 11]; the only method presented thus far.

Here we advocate that  $h \rightarrow \Upsilon\gamma$  is a good candidate to determine the sign of  $k_D$ . This occurs precisely because the cancellation is almost complete in the SM. A change in the sign of  $k_D$  means that the interference becomes constructive, thus increasing by orders of magnitude the  $h \rightarrow \Upsilon\gamma$  decay rate. This can be used to constrain the wrong-sign solution in the 2HDM.

We have performed a full simulation of the real 2HDM, including theoretical constraints from bounded from below potential [15], perturbative unitarity [16–18], oblique radiative parameters [19–21], and we keep  $m_{H\pm} > 480\text{GeV}$  to respect B-physics constraints. We include all production mechanisms [22–24] and take  $\mu_{VV}$ ,  $\mu_{\gamma\gamma}$ , and  $\mu_{\tau\tau}$  to lie within 20% of the SM, in close accordance with the latest LHC constraints [25].

The results of our simulation in the type II model are shown in Fig. 3. The red/dark-grey points pass all theoretical

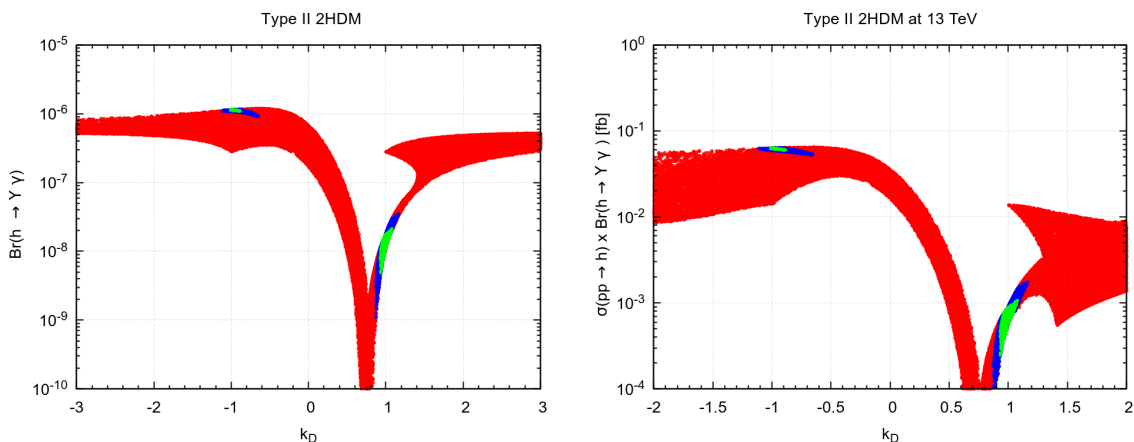


FIG. 3: Figure (a):  $\text{BR}(h \rightarrow \Upsilon\gamma)$  as a function of  $k_D$ . The red/dark-grey points pass all theoretical constraints in the type II 2HDM. The blue/black (green/light-grey) points pass both the theoretical constraints and the experimental constraints on  $\mu_{VV}$ ,  $\mu_{\gamma\gamma}$ , and  $\mu_{\tau\tau}$  at 20% (10%). Figure (b): Same plot, but for  $\sigma(pp \rightarrow h) \times \text{BR}(h \rightarrow \Upsilon\gamma)$  at 13 TeV.

constraints. The blue/black (green/light-grey) points pass those and also  $\mu_{VV}$ ,  $\mu_{\gamma\gamma}$ , and  $\mu_{\tau\tau}$  at 20% (10%). The situation for the flipped model is very similar, with only very slight differences in the allowed regions, due to the different dependence on  $\mu_{\tau\tau}$ .

There are several features of note. After theoretical constraints, the simulation allows for a very large range of  $k_D$ . Contrary to what one might naively expect, having a large  $k_D$  does not improve much the  $h \rightarrow \Upsilon\gamma$  branching ratio. The point is that, although a large  $k_D$  does indeed increase the direct amplitude, in accordance with Eq. (13), in the 2HDM the width of  $h$  is dominated by  $h \rightarrow b\bar{b}$ , which also increases with  $k_D$ . Once one introduces the experimental constraints, the values for  $k_D$  get restricted to right-sign ( $k_D \sim 1$ ) and wrong-sign ( $k_D \sim -1$ ) regions. As explained in Sec. II B, this is mostly due to  $\mu_{VV}$  and simple trigonometry [11]. Finally, one sees that, due to the same destructive interference at play in the SM, the right-sign solution leads to a minute  $h \rightarrow \Upsilon\gamma$  branching ratio around  $10^{-8}$ . In contrast, the wrong-sign solution leads to constructive interference and a  $h \rightarrow \Upsilon\gamma$  branching ratio larger by two orders of magnitude.

The possible experimental reach is best seen in Fig. 3(b), where we show a simulation of  $\sigma(pp \rightarrow h) \times \text{BR}(h \rightarrow \Upsilon\gamma)$  at 13 TeV. For the wrong-sign, we find a value around 0.06 fb. The current run II data lies around  $15\text{fb}^{-1}$  total integrated luminosity [26] and will ultimately achieve around  $100\text{fb}^{-1}$ , meaning that a measurement is becoming possible. This 0.06 fb estimate arises from the precise values taken for  $g_\Upsilon$  and the scale chosen for  $\alpha$  in the various steps of the calculation. A detailed discussion, including relativistic corrections, can be found in [13]. Our result presents a lower limit on the number of events, meaning that detection prospects are likely to be superior. Of course, an even better determination is possible at the High-Luminosity LHC, allowing for the detection or completely ruling

out of the wrong-sign solution. We have made a simulation at 14 TeV and obtain the expected increase of about 15% from 0.06 fb into around 0.07 fb, in both Type II and Flipped.

#### IV. CONCLUSIONS

The decay  $h \rightarrow \Upsilon\gamma$  is very small in the SM, due to a cancellation between the direct and indirect diagrams. In contrast, in theories with a negative  $hbb$  coupling, the interference becomes constructive and the rate is increased by orders of magnitude. We have studied this effect on the wrong-sign solution of the Type II and flipped 2HDM. We make detailed predictions for the number of events consistent with current bounds on the 2HDM and prove that searches for  $h \rightarrow \Upsilon\gamma$  constitute a viable and clean method to constrain the wrong-sign solution, especially at a high luminosity facility.

#### Acknowledgments

We are grateful to G. Bodwin for discussions and to R. Santos for carefully reading the manuscript. This work is supported in part by the Portuguese *Fundação para a Ciência e Tecnologia* (FCT) under contract UID/FIS/00777/2013.

- 
- [1] G. Aad *et al.* [ATLAS Collaboration], Observation of a new particle in the search for the Standard Model Higgs boson with the ATLAS detector at the LHC, *Phys. Lett. B* **716**, 1 (2012) [arXiv:1207.7214 [hep-ex]].
  - [2] S. Chatrchyan *et al.* [CMS Collaboration], Observation of a new boson at a mass of 125 GeV with the CMS experiment at the LHC, *Phys. Lett. B* **716**, 30 (2012) [arXiv:1207.7235 [hep-ex]].
  - [3] J. R. Espinosa, C. Grojean, M. Muhlleitner and M. Trott, First Glimpses at Higgs' face, *JHEP* **1212**, 045 (2012) doi:10.1007/JHEP12(2012)045 [arXiv:1207.1717 [hep-ph]].
  - [4] A. Falkowski, F. Riva and A. Urbano, Higgs at last, *JHEP* **1311**, 111 (2013) doi:10.1007/JHEP11(2013)111 [arXiv:1303.1812 [hep-ph]].
  - [5] G. Belanger, B. Dumont, U. Ellwanger, J. F. Gunion and S. Kraml, Global fit to Higgs signal strengths and couplings and implications for extended Higgs sectors, *Phys. Rev. D* **88**, 075008 (2013) doi:10.1103/PhysRevD.88.075008 [arXiv:1306.2941 [hep-ph]].
  - [6] J.F. Gunion, H.E. Haber, G.L. Kane and S. Dawson, *The Higgs Hunter's Guide* (Westview Press, Boulder, CO, 2000).
  - [7] G. C. Branco, P. M. Ferreira, L. Lavoura, M. N. Rebelo, M. Sher, and J. P. Silva, Theory and phenomenology of two-Higgs-doublet models, *Phys. Rept.* **516**, 1 (2012) [arXiv:1106.0034 [hep-ph]].
  - [8] A. Celis, V. Ilisie and A. Pich, Towards a general analysis of LHC data within two-Higgs-doublet models, *JHEP* **1312**, 095 (2013) doi:10.1007/JHEP12(2013)095 [arXiv:1310.7941 [hep-ph]].
  - [9] P. M. Ferreira, J. F. Gunion, H. E. Haber and R. Santos, Probing wrong-sign Yukawa couplings at the LHC and a future linear collider, *Phys. Rev. D* **89**, no. 11, 115003 (2014) doi:10.1103/PhysRevD.89.115003 [arXiv:1403.4736 [hep-ph]].
  - [10] P. M. Ferreira, R. Guedes, M. O. P. Sampaio and R. Santos, Wrong sign and symmetric limits and non-decoupling in 2HDMs, *JHEP* **1412**, 067 (2014) doi:10.1007/JHEP12(2014)067 [arXiv:1409.6723 [hep-ph]].
  - [11] D. Fontes, J. C. Romão and J. P. Silva, A reappraisal of the wrong-sign  $hb\bar{b}$  coupling and the study of  $h \rightarrow Z\gamma$ , *Phys. Rev. D* **90**, no. 1, 015021 (2014) doi:10.1103/PhysRevD.90.015021 [arXiv:1406.6080 [hep-ph]].
  - [12] G. T. Bodwin, F. Petriello, S. Stoynev and M. Velasco, Higgs boson decays to quarkonia and the  $H\bar{c}c$  coupling, *Phys. Rev. D* **88**, no. 5, 053003 (2013) doi:10.1103/PhysRevD.88.053003 [arXiv:1306.5770 [hep-ph]].
  - [13] G. T. Bodwin, H. S. Chung, J. H. Ee, J. Lee and F. Petriello, Relativistic corrections to Higgs boson decays to quarkonia, *Phys. Rev. D* **90**, no. 11, 113010 (2014) doi:10.1103/PhysRevD.90.113010 [arXiv:1407.6695 [hep-ph]].
  - [14] D. Fontes, J. C. Romão and J. P. Silva,  $h \rightarrow Z\gamma$  in the complex two Higgs doublet model, *JHEP* **1412**, 043 (2014) doi:10.1007/JHEP12(2014)043 [arXiv:1408.2534 [hep-ph]].
  - [15] N. G. Deshpande and E. Ma, Pattern of Symmetry Breaking with Two Higgs Doublets, *Phys. Rev. D* **18**, 2574 (1978). doi:10.1103/PhysRevD.18.2574.
  - [16] S. Kanemura, T. Kubota and E. Takasugi, Lee-Quigg-Thacker bounds for Higgs boson masses in a two doublet model, *Phys. Lett. B* **313**, 155 (1993) doi:10.1016/0370-2693(93)91205-2 [hep-ph/9303263].
  - [17] A. G. Akeroyd, A. Arhrib and E. M. Naimi, Note on tree level unitarity in the general two Higgs doublet model, *Phys. Lett. B* **490**, 119 (2000) doi:10.1016/S0370-2693(00)00962-X [hep-ph/0006035].
  - [18] I. F. Ginzburg and I. P. Ivanov, Tree level unitarity constraints in the 2HDM with CP violation, hep-ph/0312374.
  - [19] M. E. Peskin and T. Takeuchi, Estimation of oblique electroweak corrections, *Phys. Rev. D* **46**, 381 (1992). doi:10.1103/PhysRevD.46.381.

- [20] W. Grimus, L. Lavoura, O. M. Ogreid and P. Osland, The Oblique parameters in multi-Higgs-doublet models, Nucl. Phys. B **801**, 81 (2008) doi:10.1016/j.nuclphysb.2008.04.019.
- [21] M. Baak *et al.*, The Electroweak Fit of the Standard Model after the Discovery of a New Boson at the LHC, Eur. Phys. J. C **72**, 2205 (2012) doi:10.1140/epjc/s10052-012-2205-9 [arXiv:1209.2716 [hep-ph]].
- [22] M. Spira, HIGLU: A program for the calculation of the total Higgs production cross-section at hadron colliders via gluon fusion including QCD corrections, hep-ph/9510347.
- [23] R. V. Harlander, S. Liebler and H. Mantler, SusHi: A program for the calculation of Higgs production in gluon fusion and bottom-quark annihilation in the Standard Model and the MSSM, Comput. Phys. Commun. **184**, 1605 (2013) doi:10.1016/j.cpc.2013.02.006 [arXiv:1212.3249 [hep-ph]].
- [24] LHC Higgs cross section WG picture gallery webpage, <https://twiki.cern.ch/twiki/bin/view/LHCPhysics/LHCHXSWGCrossSectionsFigures>.
- [25] G. Aad *et al.* [ATLAS and CMS Collaborations], Measurements of the Higgs boson production and decay rates and constraints on its couplings from a combined ATLAS and CMS analysis of the LHC  $pp$  collision data at  $\sqrt{s} = 7$  and 8 TeV, arXiv:1606.02266 [hep-ex].
- [26] [https://twiki.cern.ch/twiki/bin/view/CMSPublic/LumiPublicResults#Run\\_2\\_Annual\\_Charts\\_of\\_Luminosit](https://twiki.cern.ch/twiki/bin/view/CMSPublic/LumiPublicResults#Run_2_Annual_Charts_of_Luminosit)